Ultrafast carrier dynamics at a metal-semiconductor interface

P. C. M. Christianen[a)]
High Field Magnet Laboratory and Research Institute for Materials, University of Nijmegen, Toernooiveld 1, 6525 ED Nijmegen, The Netherlands

P. J. van Hall
Physics Department, Eindhoven University of Technology, PO Box 513, 5600 MB Eindhoven, The Netherlands

H. J. A. Bluyssen[b)]
High Field Magnet Laboratory and Research Institute for Materials, University of Nijmegen, Toernooiveld 1, 6525 ED Nijmegen, The Netherlands

M. R. Leys, L. Drost, and J. H. Wolter
Physics Department, Eindhoven University of Technology, PO Box 513, 5600 MB Eindhoven, The Netherlands

(Received 20 December 1995; accepted for publication 10 September 1996)

The ultrafast carrier dynamics in the high electric field at an Au-GaAs interface has been studied experimentally as well as theoretically. The photoluminescence decay time is related directly to the carrier sweepout from the GaAs depletion region, i.e., to the time needed for photoexcited electrons and holes to leave this region. This decay time has been found to increase drastically with laser input power, ranging from a few picoseconds at low excitation to values of 10–20 ps at high excitation. These results indicate a significant retardation of the sweepout, which cannot be explained by intervalley scattering and space-charge effects. From our Monte Carlo calculations it has been found that the applied electric field collapses totally almost instantaneously after laser excitation due to the enormous excess of photoexcited charges. The sweepout only recovers after some time needed to recharge the device. © *1996 American Institute of Physics.* [S0021-8979(96)05924-5]

I. INTRODUCTION

The study of the ultrafast dynamics of hot carriers in semiconductors in high electric fields is important not only for designing structures for high speed optoelectronics but also for the fundamental understanding of energy relaxation and non-linear transient transport. Originally investigations concerning the ultrafast non-stationary and non-equilibrium carrier transport have been restricted to theoretical predictions, due to the lack of experimental techniques.[1] However, since the availability of picosecond (and more recently of femtosecond) light sources a large number of time-resolved investigations have been carried out to check the predicted ultrafast behavior of carriers. Recently, several groups have employed successfully a photoconductivity technique,[2] using (sub)picosecond laser pulses and fast optical switches to measure the transient transport. They have used Monte Carlo calculations in an attempt to understand the results.[3–5] Experimental evidence for a velocity overshoot in GaAs, as predicted first by Ruch,[6] has been found to occur for electrons photoexcited into the Γ-valley of the conduction band in a biased GaAs photoconductor. The electrons are accelerated in the Γ-valley due to the high electric field. Above a certain field strength the electrons gain enough energy to be scattered into the satellite L-valley, resulting in a lower drift velocity.[4] Photoexcitation closer to the conduction band-edge results in a larger velocity overshoot, because the electrons spend more time in the Γ-valley, before they scatter into the satellite valleys. These effects which are due to the inherent band structure and intervalley scattering should not be confused with the transport transients arising from space-charge-separation effects.[5] Since the photoexcited electrons and holes drift in opposite directions the internal electric field is changing, which can produce a photoconductive transient as well. Furthermore in practice the non-linear transient carrier transport in a real device might also be strongly affected by additional phenomena, such as the influences of the contacts and an electric field depending on time and position.

Therefore we investigate the ultrafast carrier dynamics in the high intrinsic electric field at a metal-semiconductor interface, in order to gain insight into which of the above mentioned parameters determine the transient transport.

The carrier sweepout from the depletion region of a modified biased Au-GaAs Schottky barrier was studied with use of a subpicosecond photoluminescence correlation technique.[7] The use of this technique in this kind of experiment, as applied first by Von Lehmen *et al.*,[8,9] offers the possibility to monitor the carrier transport on a subpicosecond time scale. Moreover, in principle this technique can provide for energy-resolved correlated photoluminescence spectra in order to probe the energy distribution and the energy relaxation of the carriers.

This paper is organized as follows. In the next section the layer composition of the modified Schottky barrier will be discussed, which is of major importance for the total photoluminescence yield. Subsequently the experimental results will be presented in Section III. In order to understand the experimental results a set of Monte Carlo simulations has

a)Electronic mail: peterc@sci.kun.nl
b)Present address: High Magnetic Field Laboratory, Max-Planck-Institut für Festkörperforschung and Centre National de la Recherche Scientifique, BP 166, F-38042 Grenoble Cedex 9, France.

 0021-8979/96/80(12)/6831/8/$10.00

	⇓		laser excitation
80 Å	Au		metal
100 Å	GaAs	undoped	caplayer
100 Å	$Al_{.4}Ga_{.6}As$	undoped	
.3 μm	n-GaAs	$10^{17} cm^{-3}$	depletion layer
100x	50 Å GaAs/ 50 Å $Al_{.33}Ga_{.67}As$ n-type	$10^{18} cm^{-3}$	superlattice buffer
	n^+-GaAs		substrate
	Au-Ge-Ni contact		

FIG. 1. Layer composition of the modified Schottky barrier.

been performed, of which the ingredients and assumptions will be discussed in Section IV. In Section V the results of the calculations will be compared with the experimental observations. Finally, the conclusions will be summarized in the last section.

II. SAMPLE COMPOSITION

The experiments were performed on modified Schottky barrier samples, grown by molecular beam epitaxy. The layer composition is shown schematically in Figure 1. The actual barrier is formed by a 0.3-μm-thick n-type GaAs (doping concentration: 10^{17} cm^{-3}) layer and a semitransparent Au film of 80 Å thickness, to allow for laser excitation through the metal top contact. To suppress interface recombination and provide for a superior optical quality the sample contains a very thin (100 Å) undoped $Al_{0.4}Ga_{0.6}As$ layer between the metal and the depletion layer, capped by a 100-Å-thick undoped GaAs layer. In addition a heavily doped n-type (doping concentration: 10^{18} cm^{-3}) superlattice buffer layer (100 × 50 Å GaAs/50 Å $Al_{0.33}Ga_{0.67}As$) has been inserted between the depletion layer and the n^+-GaAs substrate. This superlattice prevents carrier creation in the substrate which could cause a disturbing background signal in addition to the depletion layer photoluminescence. The size of the sample amounts to 4 × 4 mm^2. A voltage bias can be applied across the sample between a AuGeNi backside contact and the top Au contact. The insertion of the (Ga,Al)As layer at the top and the superlattice at the bottom was found to leave the current-voltage characteristics unchanged for reverse biases. Capacitance-voltage measurements indicated a

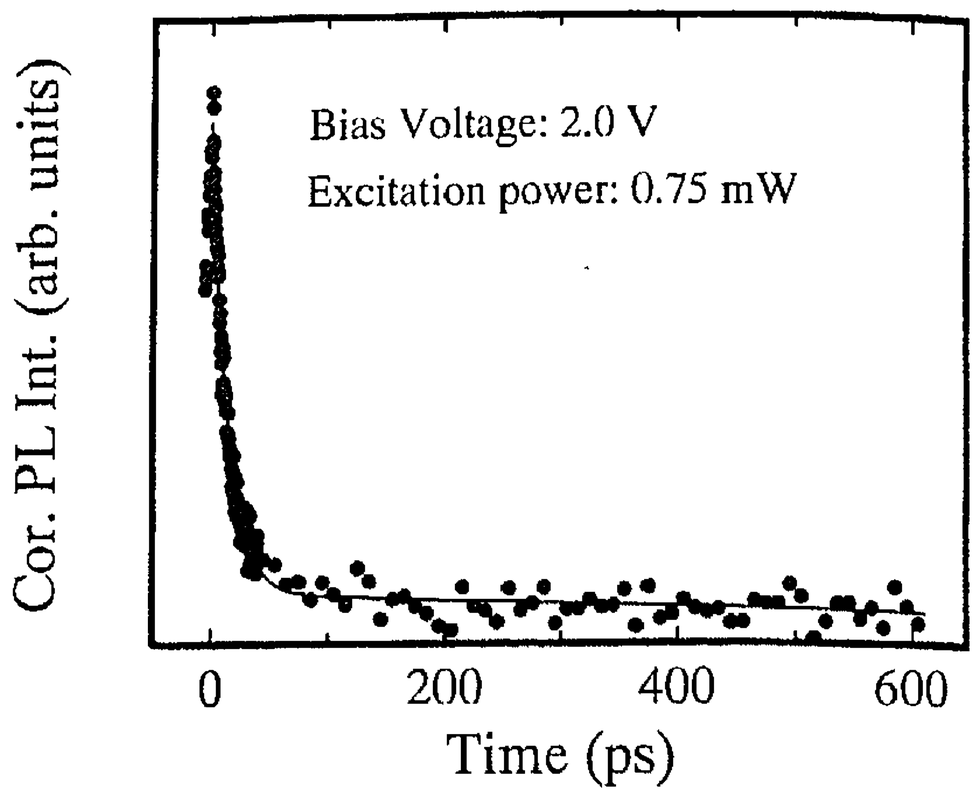

FIG. 2. Typical correlated photoluminescence (PL) intensity as function of the time delay between the pulses. The solid curve corresponds to a fit according to Equation (2).

value for the Schottky barrier height of 0.90 V and a capacitance per area of 5.2 × 10^{-4} F m^{-2} at 3 V reverse bias.

III. THE EXPERIMENT

Subpicosecond time-resolved photoluminescence measurements were performed with help of a correlation technique.[7] The sample was excited by two laser pulse trains (generated by a colliding pulse mode dye laser, pulse width 60 fs, energy 2.03 eV, repetition rate 100 MHz) of equal amplitude, with a variable time delay δt in between. The two beams were chopped separately at frequencies ω_1 and ω_2 and were focused to a 20 μm diameter spot onto the sample surface. The time-integrated photoluminescence of the depletion layer was guided through a 1 m monochromator (Monospek) and detected by a cooled GaAs photomultiplier with use of a lock-in amplifier tuned to frequency ω_1-ω_2. The resulting photoluminescence signal can be expressed as the cross correlation of the electron (n_i) and hole (p_i) populations, photoexcited by the first ($i=1$) and second ($i=2$) laser pulses:

$$I(\delta t)=\int [n_1(t)p_2(t+\delta t)+n_2(t+\delta t)p_1(t)]\mathrm{d}t. \qquad (1)$$

The signal is determined by the overlap in both real space and **k** space of the electron and hole distributions inside the GaAs depletion region. Thus the decay of the photoluminescence intensity is a measure for the ultrafast transport of the carriers.

This correlated photoluminescence intensity was measured at an energy close to the band edge, as a function of the reverse bias across the sample ($0 \leqslant V_{\text{bias}} \leqslant 4.0$ V), i.e., the backside contact is positively charged with respect to the top contact. Also the laser excitation power was varied from 0.1 mW to 2.0 mW, that is the concentration of created carriers ranged from less than 5×10^{16} to more than 5×10^{17} cm^{-3}.

A typical correlation trace for the entire time interval used ($\delta t \leqslant 600$ ps) is depicted by dots in Figure 2 for a reverse bias of 2.0 V and an excitation power of 0.75 mW. It is clear that the photoluminescence decay is composed of a

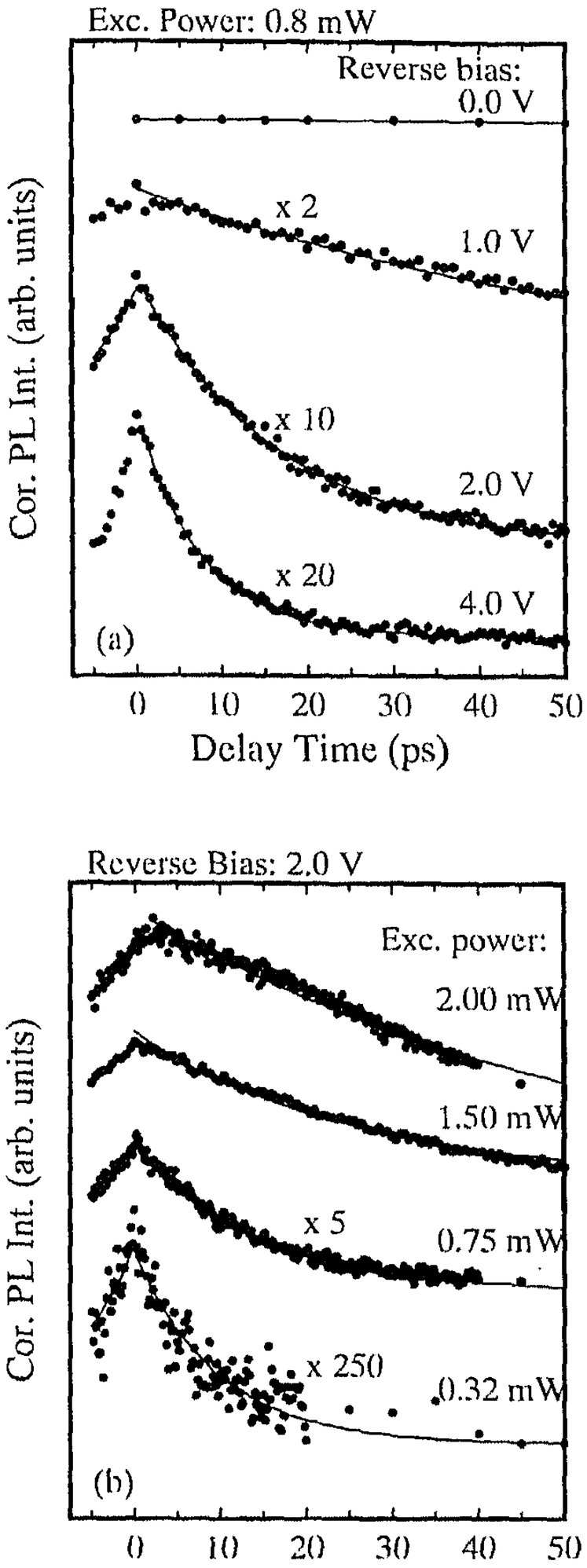

FIG. 3. Correlated photoluminescence (PL) intensity as function of time delay between the pulses for different reverse bias voltages (a) and excitation powers (b). The solid curves correspond to the best fits to the data. Some of the traces are vertically shifted and multiplied by the given numbers for clarity.

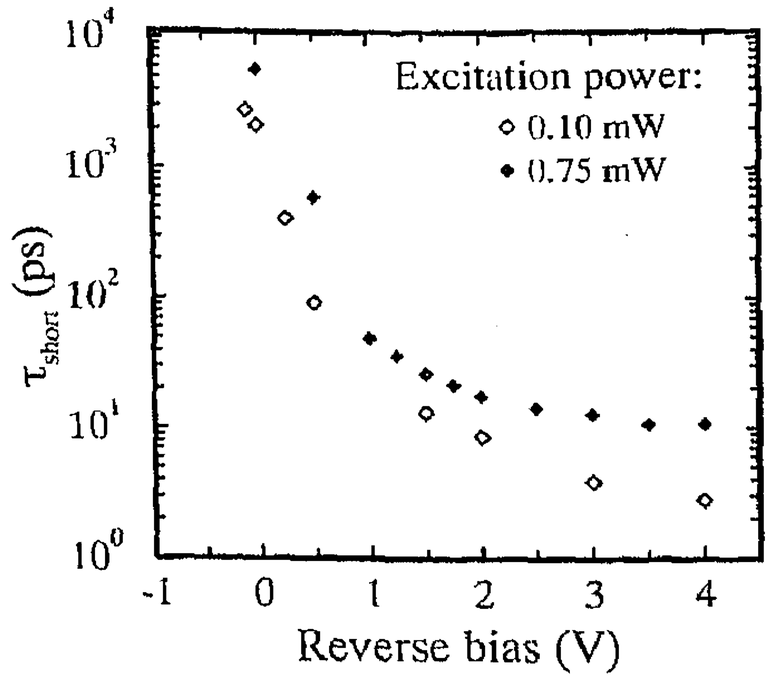

FIG. 4. Short correlated photoluminescence (PL) decay times as function of reverse bias voltage for input powers 0.1 mW (open triangles) and 0.75 mW (filled triangles). The values are obtained by fitting the experimental correlation curves to expression (2).

and the resulting values of the fast decay times τ_{short}, are shown in Figures 4 and 5, for a variety of reverse bias voltages and input powers respectively.

The main features to be noted are the following. With increasing reverse bias voltage (Figure 4) the photoluminescence decay time reduces drastically over three orders of magnitude, from several nanoseconds at zero bias voltage to a few picoseconds at 4.0 V reverse bias voltage. For the lowest reverse bias voltages (<0.2 V) the depletion width of the Schottky barrier was estimated to be considerably thinner (~ 0.1 μm[10]) than the total active GaAs layer thickness (0.3 μm). Therefore the decay time approaches the spontaneous carrier lifetime, since the photoluminescence decay is determined mainly by carriers in the flat band region. With increasing reverse bias both the depletion width as well as the internal electric field increase, leading to a considerably faster carrier sweepout, which results in decay times as small as 3 ps under favorable conditions. This time constant agrees with the results of Von Lehmen *et al.*,[9] who assigned it to electrons traversing the depletion region at their saturation velocities. In addition, the decay time increases with increasing excitation power. For instance for 3.0 V and 4.0 V reverse bias voltage the decay time grows from a few picosec-

rapidly and a slowly decaying component. Therefore the experimental data were fitted to the sum of two exponential functions, according to:

$$I(\delta t)=A_{\text{short}}\exp\left[-\frac{\delta t}{\tau_{\text{short}}}\right]+A_{\text{long}}\exp\left[-\frac{\delta t}{\tau_{\text{long}}}\right]. \qquad (2)$$

The solid curve in Figure 2 represents this fit. The contribution to the signal with the long time constant hardly decays within the time interval used. But the short decay time, which we attribute to the carrier sweepout from the GaAs depletion layer, strongly depends on reverse bias and excitation power. This can be seen in Figure 3, which shows typical measured correlation curves for different applied reverse bias voltages [Figure 3(a)] and excitation powers [Figure 3(b)]. The solid curves correspond to fits using Equation (2),

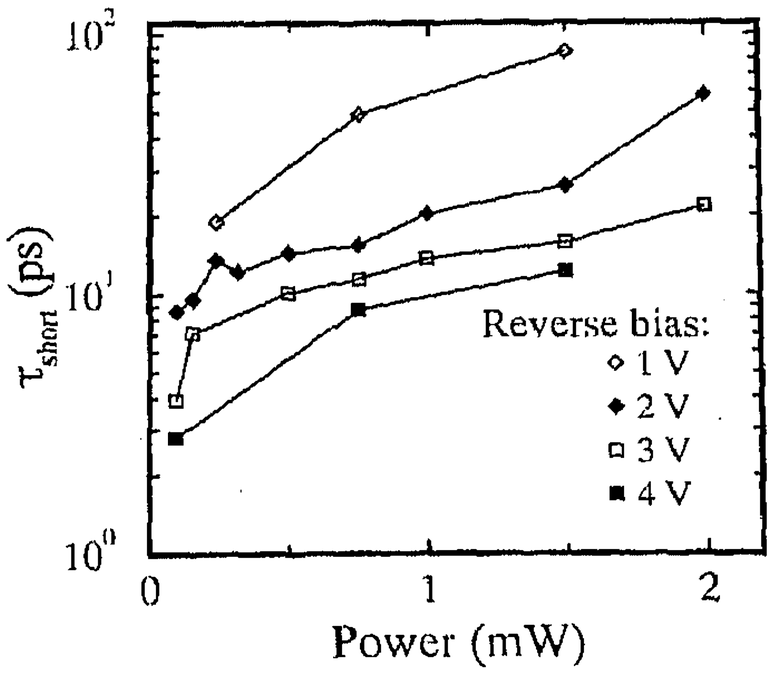

FIG. 5. Short correlated photoluminescence (PL) decay time as function of excitation power for a number of reverse bias voltages. The values were obtained by fitting the experimental correlation curves to expression (2).

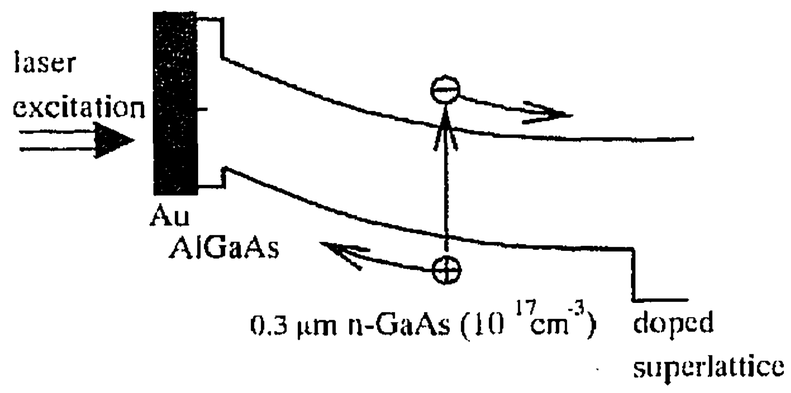

FIG. 6. Schematic representation of the band bending at the metal-semiconductor interface, without carrier injection, used as initial potential in the Monte Carlo simulations.

onds at 0.1 mW to a significantly higher value of about 10–20 ps at 2.0 mW excitation power (Figure 5).

In addition to the rapidly decaying correlated photoluminescence contribution another component is present, which hardly decays within the time interval used (Figure 2). A reliable determination of its time constant τ_{long} would require an extension of the measurements towards longer delay times. From the present experimental results τ_{long} was estimated to amount to several nanoseconds, within the experimental error independent of the parameters varied. Moreover, also the normalized coefficient A_{long} of this slowly decaying component did not vary strongly with bias voltage or input power. For the origin of this component a few explanations are possible:

(i) despite the precaution taken by growing the superlattice buffer, carriers were created in the substrate causing a disturbing luminescence background.
(ii) luminescence emitted by carriers created in the 100-Å-thick GaAs caplayer.
(iii) photoluminescence emission due to carriers which were left behind in the depletion layer after the first carrier sweepout because of the built-in potential barriers, i.e. the intermediate AlGaAs layer and the superlattice buffer layer for low-energetic holes or electrons respectively.

To our opinion the lack of a distinct dependence on the experimental parameters suggests that this part of the signal originated from the region which was the least affected by the bias voltage, i.e. the substrate.

IV. THE MONTE CARLO SIMULATIONS

In order to find an interpretation of the presented experimental results Monte Carlo simulations were performed. Special attention was paid to the striking retardation of the carrier sweepout in the case of a high laser input power.

In these simulations the device was modeled schematically assuming an initial band bending at the metal-semiconductor interface as is indicated in Figure 6. The 0.3-μm-thick GaAs layer is separated from the Au by a barrier formed by the intermediate AlGaAs layer and the Schottky barrier. Due to its heavy n-type doping the superlattice was assumed to form no barrier for the electrons and a large one for the holes. The applied bias voltage creates an interface charge at the Au film which is compensated for by a constant intrinsic space-charge throughout the whole depletion layer giving rise to a linear decreasing electric field and a parabolic potential (Figure 6). This means that in this model the depletion width was constant and equal to the GaAs layer thickness, whereas the doping concentration was varied with the applied bias voltage. In an actual Schottky device the doping level is constant and the depletion width changes with bias voltage.[10] Although this model is rather schematic we believe it nevertheless contains the basic physics needed for describing semi-quantitatively the experimental results for the high reverse bias voltages ($>$2.0 V), when the depletion region approaches the GaAs layer thickness.

The carriers were created in the depletion layer according to the absorption coefficient of GaAs for the laser light. The subsequent transport and energy relaxation of both electrons and holes in the GaAs layer were computed in a Monte Carlo simulation,[11] accounting for the various scattering mechanisms such as optical and acoustic phonon-, ionized impurity-, intervalley-, and carrier-carrier scattering.[12,13] Both electron-heavy- and -light-hole pairs were considered, including hole interband transitions.[14] Standard 10^4 electron-hole pairs were used. In some cases the statistical accuracy of the results was checked with simulations using 10^5 electron-hole pairs.

The correlated photoluminescence signal was calculated according to Equation (1), making two simplifying assumptions in order to keep the problem manageable:

(i) the carrier distributions excited by both pulses were the same, but shifted in time. Thus the effect of the second pulse arriving at the sample whose features (e.g. absorption, local electric field) may be changed by the carriers of the first pulse, was neglected.
(ii) the distribution in **k** space was taken to be independent of the real space position inside the device. A scaling factor, which represents the integral over **k** space, counted the number of carriers at each position.

Evidently photoexcitation of charged particles may give rise to a space-charge field. Directly after excitation, when the electrons and holes are still close to each other this field is zero. However, as soon as the electrons and holes start to move as a result of the applied field, a counteracting electric field will build up. To account for this space-charge effect, which can be especially large for the highest intensities used, the Poisson equation was solved in one dimension every 1 fs of the calculation, resulting in a time-dependent local driving field, i.e. time-dependent energy band profile, in addition to the applied field.

An additional important point to note is the following. The pronounced input power dependence of the experimental results suggests that the photoexcited charge dominates the charge initially present in the biased device. Therefore it is worthwhile to consider the situation in more detail. In the case of the highest input power the photoinjected charge is still four orders of magnitude lower that the total charge on the device. However, it is the charge density, i.e. the charge on the illuminated part, that is important and not the total charge present on the device (see Figure 7). For example the photoexcited charge density can exceed the intrinsic one by a factor of 20, inevitably leading to serious consequences for

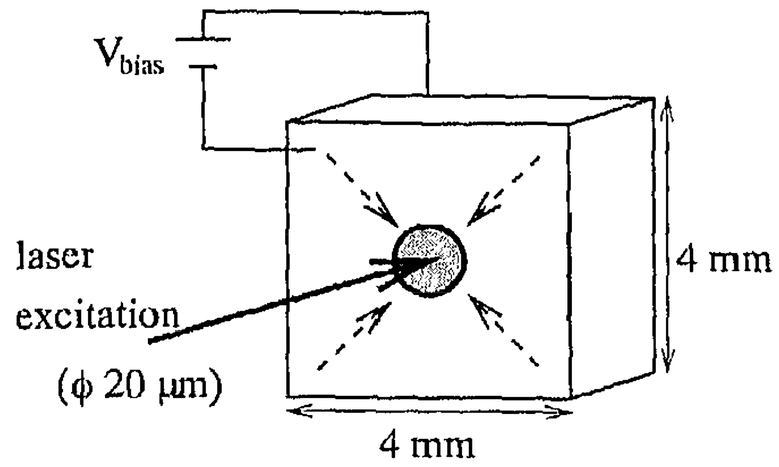

FIG. 7. Schematic representation of the charge flow in the top contact directly after excitation, which is governed by the so-called regeneration time τ_{reg}.

the carrier sweepout, as will be shown in the following.

Very shortly after excitation a number of holes will reach the top contact, where these holes neutralize the metal surface charge, leading to a reduced field strength. In the case that the photoexcited charge density significantly exceeds the intrinsic one, the applied field may be destroyed totally by only a small part of the excited holes. It will take some time before the field will be restored, that is the time needed to recharge that part of the device which is decharged, i.e. the illuminated part, as is illustrated in Figure 7. Obviously this recharging time is related to the *RC*-time constant of the device studied, which is basically the illuminated part incorporated in the total device on which a surplus of charge is present. From *C-V* measurements the capacitance of the illuminated part was estimated to be about 0.2 pF. The resistance was believed to be determined by the very thin semi-transparent top Au contact which has a square resistance of a few ohms, rather than the low ohmic highly doped backside contact. As a result the *RC*-time was expected to be about 1.0 ps. In order to investigate the consequences for the carrier sweepout of such a recharging time, we introduced a so-called regeneration time constant τ_{reg} by which charge is transferred to the illuminated part of the top contact tending to keep the total voltage across the depletion layer constant. In practice the positive charge reaching the top contact was compensated for by adding negative charge with a time constant τ_{reg} in order to keep the effective bias constant. However, it should be noted that also in the case holes are stuck in the band bending region, e.g. at the built-in barrier due to the intermediate AlGaAs layer (Figure 6), an extra amount of charge has to be transferred to the top contact in order to keep this voltage at its original value.

V. THEORETICAL RESULTS AND DISCUSSION

The calculations were performed for reverse bias voltages of 1.5 V and 3.0 V, i.e. average fields of 50 kV/cm and 100 kV/cm respectively, input powers ranging from 0.1 to 2.5 mW, and a number of regeneration times in the range 0–1.0 ps. Figure 8 shows the typical occupation of the Γ (a) and the *L* valley (b) of the conduction band as a function of the time and the position calculated for a voltage of 3.0 V, a laser input of 1.0 mW and a regeneration time of 1.0 ps. Directly after excitation at $t=0$ the Γ-valley occupation throughout the depletion region drops significantly, which is primarily the result of intervalley scattering as can be seen by

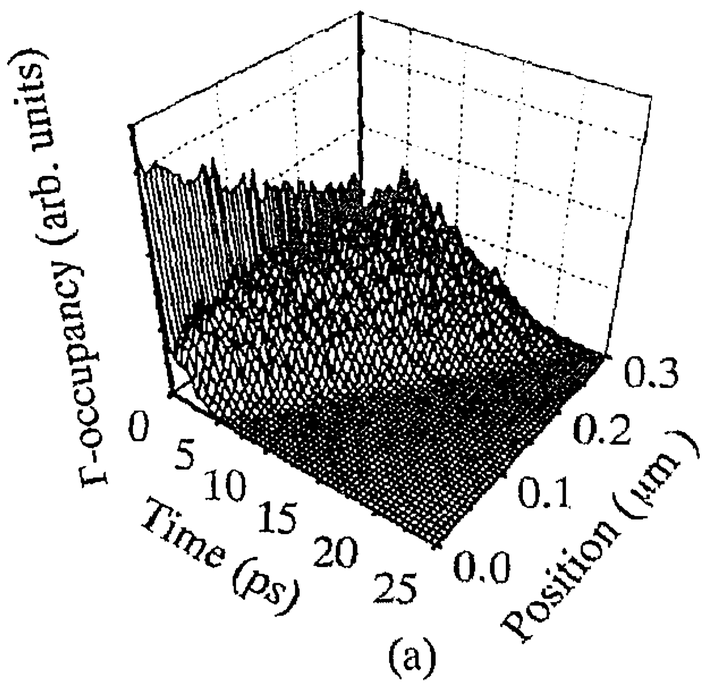

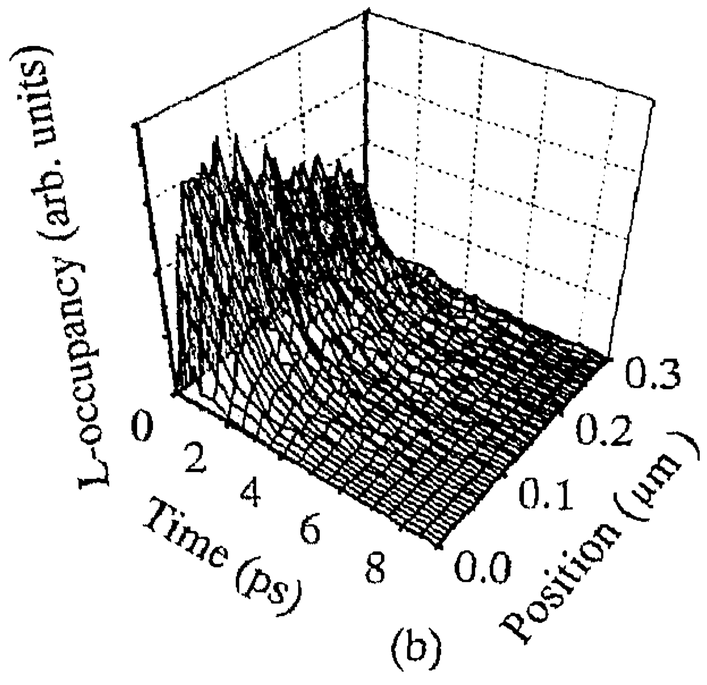

FIG. 8. Calculated time- and spatial-dependent occupancy of the Γ (a) and *L* valleys (b) of the conduction band. A position of 0.0 μm corresponds to the top Au contact. The calculations were performed for a 3 V bias and 1 mW excitation power.

the high *L*-valley occupancy at short times. The electrons were created by a 2.03 eV laser pulse and therefore have an excess energy larger than the energy of the *L*- and *X*-satellite valleys. As a result of the large effective mass of the satellite valleys and their degeneracy the photoexcited electrons are very efficiently scattered into these valleys.[15,16] The scattered electrons relax to the bottom of the satellite valley and scatter back to the central valley on a picosecond time scale, causing a global maximum of the Γ occupation around a few picosecond time delay. The Γ-valley spatial distribution shifts gradually towards the backside contact driven by the electric field, on a time scale of 10 ps. Evidently this time depends strongly on the actual experimental parameters. In order to make a proper comparison between the calculated and measured sweep out times we calculated the correlated photoluminescence intensity according to Equation (1) from the electron and hole distributions in space and time. Figure 9 shows the result for the time-dependent electron-heavy-hole recombination, for low (a) and high (b) input powers and various regeneration times at a bias of 3.0 V. The photoluminescence intensity due to electron-light-hole recombination appeared to be one order of magnitude smaller. It is evident that in all cases with $\tau_{reg}=0$, i.e. the recharging was given infinite speed to keep the voltage across the depletion layer constant, the photoluminescence decay time and thus the carrier sweepout is the fastest. Even for the lowest excitation power (0.1 mW) already a noticeable reduction of the correlated photoluminescence decay rate is visible, whenever

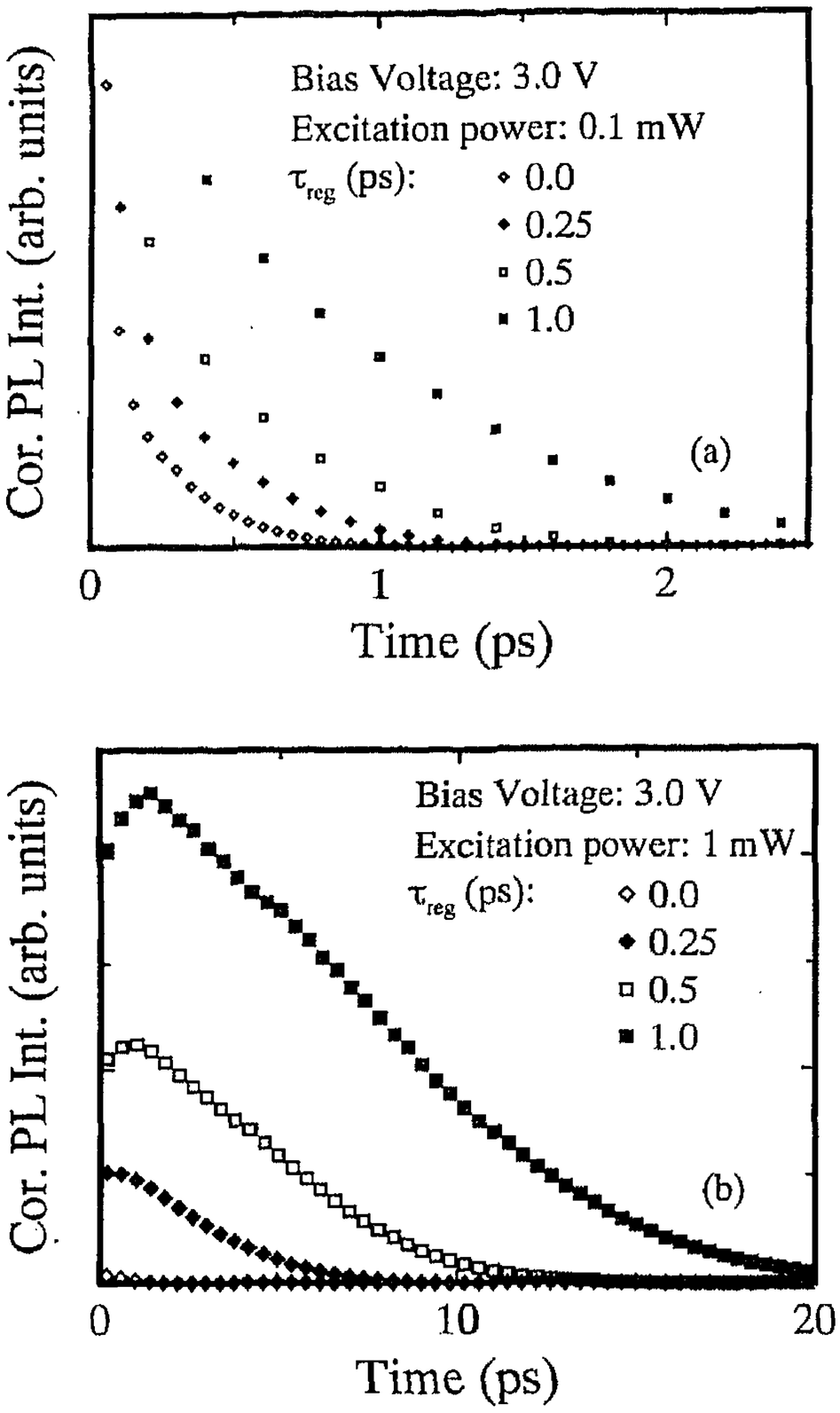

FIG. 9. Calculated correlated photoluminescence (PL) decay curves for a bias voltage of 3.0 V and the input powers 0.1 mW (a) and 1.0 mW (b) for a number of values for the regeneration time τ_{reg}.

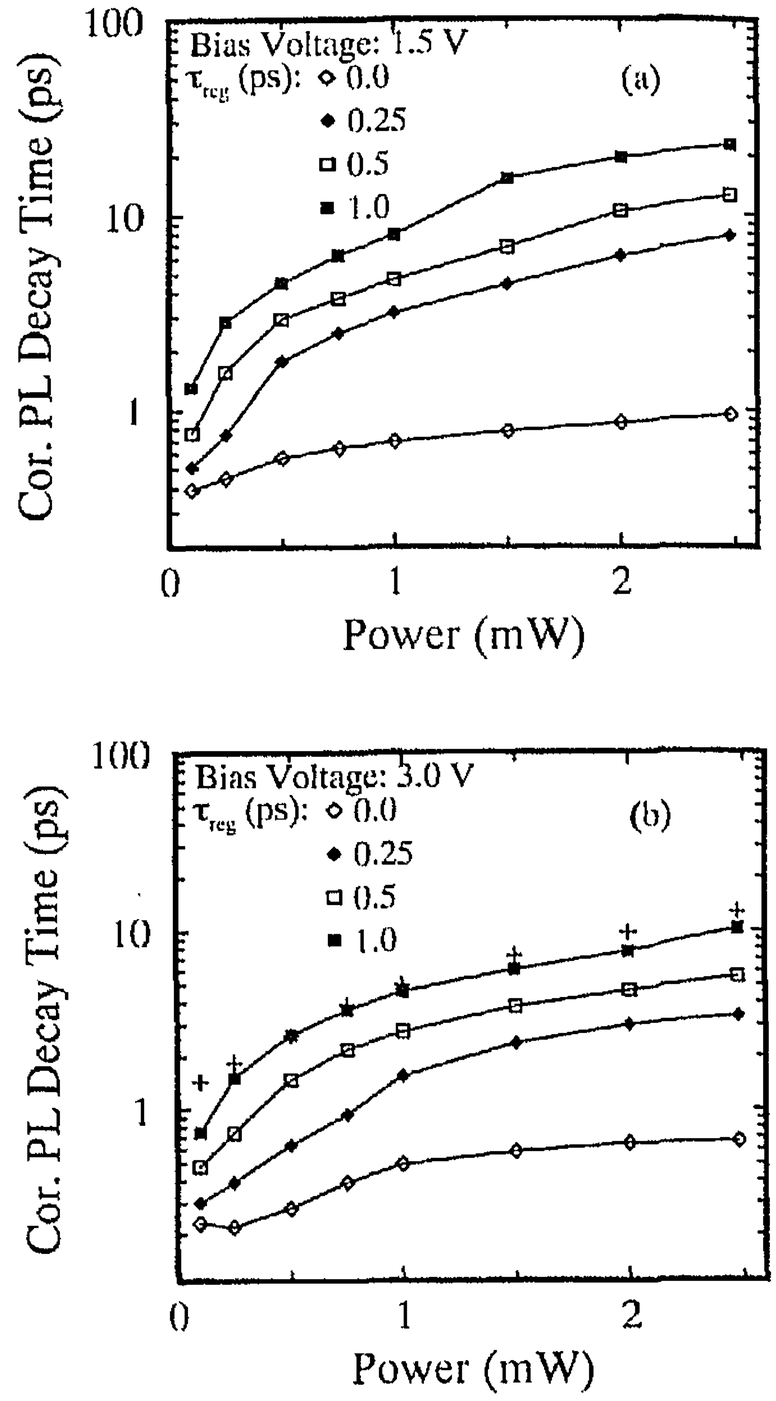

FIG. 10. Calculated photoluminescence (PL) correlation decay times for 1.5 (a) and 3.0 V (b) bias voltage, as function of the input power and various regeneration times. The pluses in (b) reflect the results of a more realistic Monte Carlo simulation.

$\tau_{reg} \neq 0$. For the higher input power the reduction in the photoluminescence decay rate becomes enormous. It is striking that the introduction of a regeneration time which is still considerably small ($\tau_{reg} \leqslant 1.0$ ps), already can retard the carrier sweepout up to time scales of ten picoseconds, in the case of the highest input powers. This can be traced back directly to the enormous excess of photoexcited charge density. Ultimately, the measured carrier sweepout depends not only on the regeneration time but also on the photoexcited charge density.

Figure 10 summarizes the calculated photoluminescence correlation decay time as a function of input power, for a number of bias voltages and regeneration times. The results for an infinitely fast regeneration time ($\tau_{reg}=0$) indicate some retardation of the carrier sweepout with input power, determined completely by space-charge effects. Obviously for this case the calculated decay times appear much too small with respect to the experimental observations. The discrepancy between the experiment and these first calculations can be solved by the introduction of one single time constant τ_{reg}, which represents a device recharging time. For all input powers the decay times get considerably longer with increasing τ_{reg}. Note that the calculated decay times for a regeneration time of 1.0 ps are in reasonable quantitative agreement with the experimental results (Figure 5). Furthermore the calculated decay times for the higher bias voltage (3.0 V) are shorter than for the lower bias voltage (1.5 V) in agreement with the results of Figure 4. However, the assumption in the model of a homogeneous space charge for all bias voltages, rather than a bias dependent depletion region width, makes a detailed comparison not possible for low voltages.

Evidently the amount of photoexcited charge is of crucial importance for the actual sweepout. It is therefore interesting to see what happens to the effective bias across the depletion region after intense laser excitation.

Figure 11 depicts the time evolution of the effective bias for an initial bias voltage of 3.0 V, 1.0 mW input power and for different values of the regeneration time τ_{reg}.

It is clear that directly after excitation the effective bias is destroyed completely due to the neutralization of the metal surface charge by the photoexcited holes that reach the top contact. Note that the effective bias may even be inverted for some time, which is caused by the inertia of the carriers moving to the contacts. Obviously the speed of the recharging process depends on the value of the regeneration time, that is, the longer the regeneration time the longer the effective bias remains destroyed. In the absence of the electric field, a large number of electrons is returning from the satellite valleys to the Γ valley, while in addition the carrier sweepout from the depletion region is delayed. Both effects give rise to a considerable enhancement of the photoluminescence decay time.

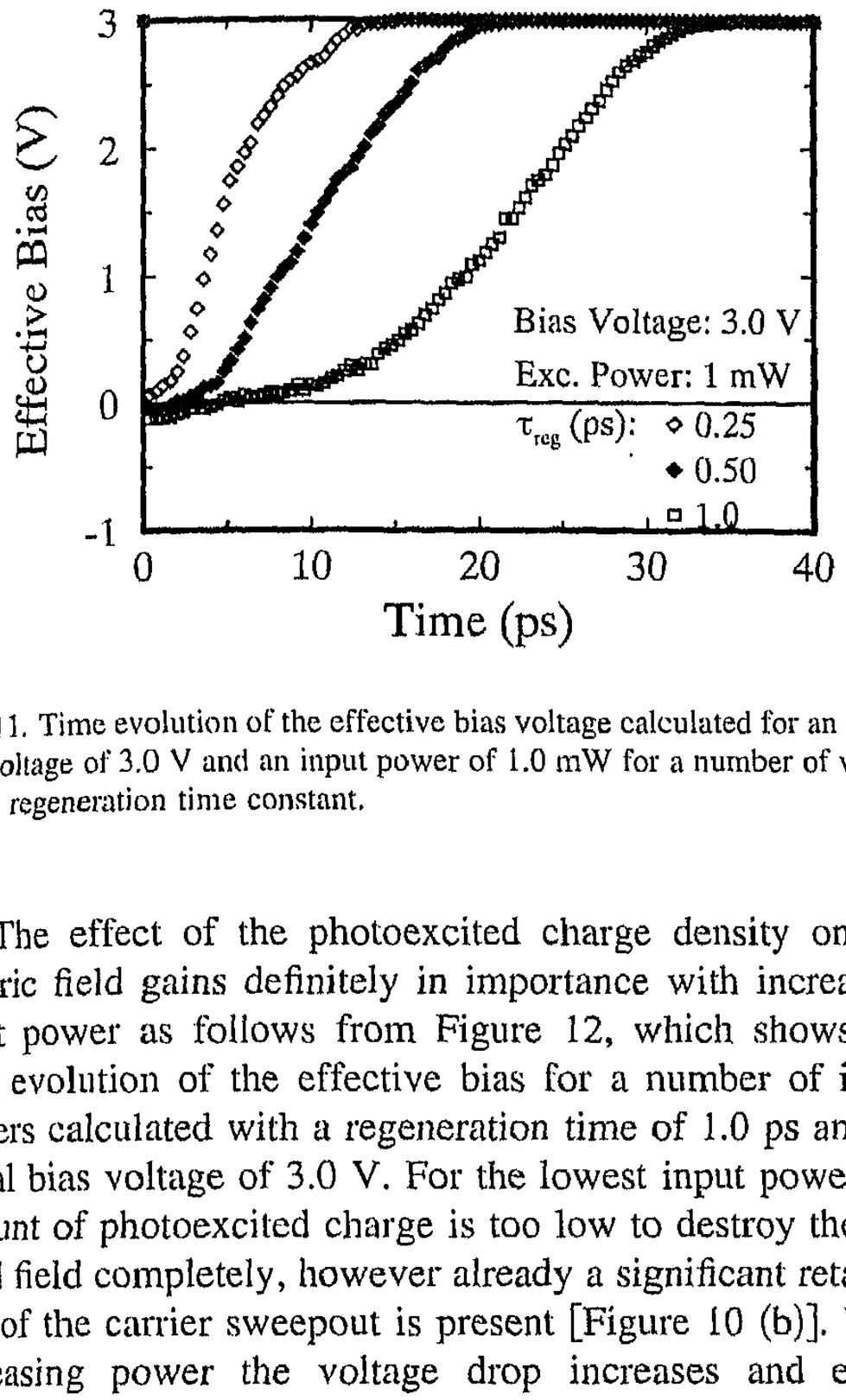

FIG. 11. Time evolution of the effective bias voltage calculated for an initial bias voltage of 3.0 V and an input power of 1.0 mW for a number of values of the regeneration time constant.

The effect of the photoexcited charge density on the electric field gains definitely in importance with increasing input power as follows from Figure 12, which shows the time evolution of the effective bias for a number of input powers calculated with a regeneration time of 1.0 ps and an initial bias voltage of 3.0 V. For the lowest input power the amount of photoexcited charge is too low to destroy the applied field completely, however already a significant retardation of the carrier sweepout is present [Figure 10 (b)]. With increasing power the voltage drop increases and exists longer, resulting in the extraordinary long photoluminescence decay times observed experimentally.

In view of the schematic modeling of the device and the two assumptions made in the calculation of the correlation functions the agreement between experiment and calculations should be considered as very satisfactory. The first assumption is the most critical one since the second pulse creates its electron-hole pairs in the situation of a collapsed field. To investigate this point, more realistic (time consuming) Monte Carlo simulations were performed in which the effect of the two incident pulses were not equal, for the situation of 3 V bias and a τ_{reg} of 1 ps. The extracted decay times are given as pluses in Figure 10. Generally there is a very good agreement between the two calculations, except perhaps for the lowest input powers. It should be noted that these more sophisticated calculations makes the agreement with the experiment (photoluminescence decay time equals 3 ps) for the lower input powers slightly better. Moreover, from these more realistic simulations it appears that the maximum in the correlated photoluminescence intensity around 1 ps [Figure 9 (b)] is merely an artifact which disappears in the calculations without the first assumption.

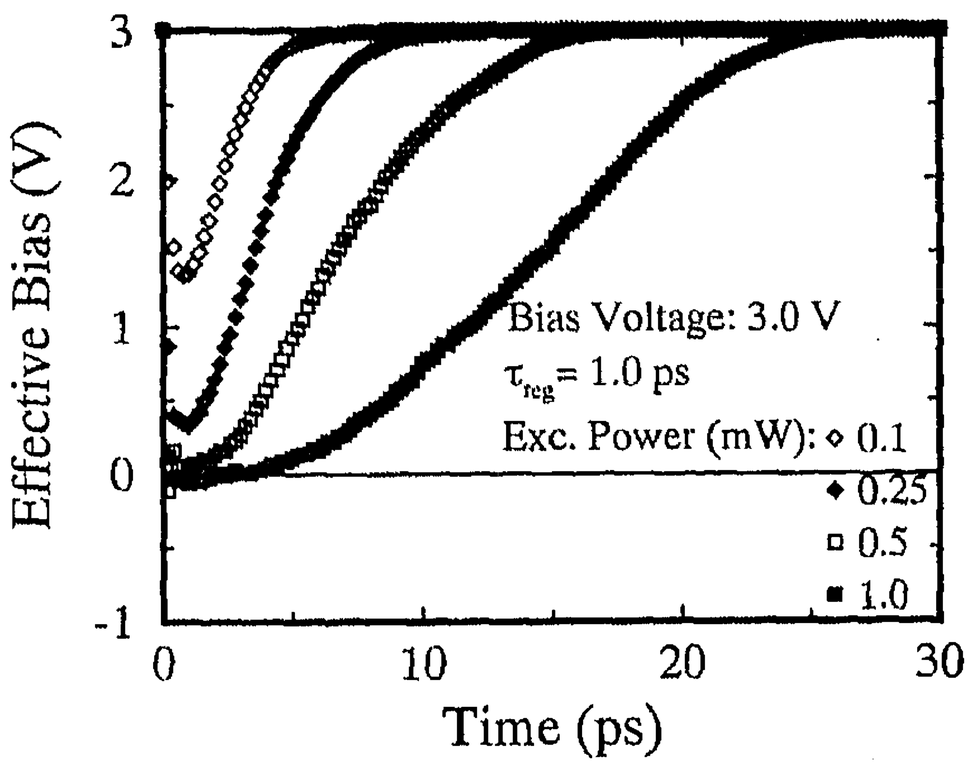

FIG. 12. Time evolution of the effective bias voltage, calculated for an initial bias voltage of 3.0 V and a regeneration time of 1.0 ps for a number of input powers.

Finally we may conclude that our interpretation of the retarded sweepout is correct. Consequently it should be emphasized that in order to determine or examine sweepout phenomena in these kind of optoelectronic structures the photoexcited carrier densities should be kept very low to avoid excess charge effects.

VI. CONCLUSIONS

In summary, the ultrafast carrier sweepout from the depletion region of a Au-GaAs Schottky barrier has been found to be strongly affected by the external conditions, which might act as an extra limit for operating a device at its maximum frequency or which might lead to peculiar highly non-linear transport transients. Since even at moderate laser input powers the injected charge density dominates the one initially present, the applied field collapses almost instantaneously after laser excitation, while its reconstruction takes the time needed to recharge the device. A contact recharging time constant had to be invoked in the Monte Carlo analysis to explain the experimental observations. The use of a recharging time of 1 ps, which corresponds to the estimated device RC time, leads to the nice quantitative reproduction of the experimentally observed carrier sweepout. Ultimately the actual carrier sweepout is determined by both the contact regeneration time and the photocreated carrier concentration. In view of the common values of the electric fields involved and the laser input levels used, it should be noted that the concept of a finite time for the restoration of the internal electric field should be applicable to other optoelectronic devices as well, for example fast optoelectronic switches.[17]

ACKNOWLEDGMENTS

The authors wish to thank A. F. van Etteger and C. A. van 't Hof for their expert technical assistance. Part of this work was supported by the "Stichting voor Fundamenteel Onderzoek der Materie" (FOM) with financial support of the "Nederlandse Organisatie voor Wetenschappelijk Onderzoek" (NWO).

[1] D. K. Ferry, H. L. Grubin, and G. J. Iafrate, in *Semiconductors Probed by Ultrafast Laser Spectroscopy*, edited by R. R. Alfano (Academic, New York, 1984).
[2] D. H. Austin, Appl. Phys. Lett. **26**, 101 (1975).
[3] R. B. Hammond, Physica B **134**, 475 (1985).

[4] K. Meyer, M. Pessot, G. Mourou, R. Grondin, and S. Chamoun, Appl. Phys. Lett. **53**, 2254 (1988).
[5] A. Evan Iverson, G. M. Wysin, D. L. Smith, and A. Redondo, Appl. Phys. Lett. **52**, 2148 (1988).
[6] J. G. Ruch, IEEE Trans. Electron Devices **ED-19**, 652 (1972).
[7] D. Rosen, A. G. Doukas, Y. Badanski, A. Katz, R. R. Alfano, Appl. Phys. Lett. **39**, 935 (1981); D. Rosen, A. G. Doukas, A. Katz, Y. Budanski, and R. R. Alfano, in Ref. 1, pp. 393–407.
[8] A. Von Lehman and J. M. Ballantyne, Appl. Phys. Lett. **44**, 87 (1984).
[9] A. Von Lehman and J. M. Ballantyne, Appl. Phys. Lett. **45**, 767 (1984).
[10] S. M. Sze, *Physics of Semiconductor Devices*, 2nd ed. (Wiley, New York, 1981).
[11] C. Jacoboni and L. Reggiani, Rev. Mod. Phys. **55**, 645 (1983).
[12] C,. Jacoboni and P. Lugli, in *The Monte Carlo Method for Semiconductor Device Simulation* (Springer, New York, 1989).
[13] *Hot Electron Transport in Semiconductors*, edited by L. Reggiani (Springer, New York, 1985).
[14] M. Costato and L. Reggiani, Phys. Status Solidi B **58**, 461 (1973).
[15] J. Shah, B. Deveaud, T. C. Damen, W. T. Tsang, A. C. Gossard, and P. Lugli, Phys. Rev. Lett. **59**, 2222 (1987).
[16] D. Y. Oberli, J. Shah, and T. C. Damen, Phys. Rev. B **40**, 1323 (1989).
[17] L. Drost, Master's thesis, Eindhoven University of Technology, 1994 (in Dutch).